

Article

The Influence of Various Solar Radiations on the Efficiency of a Photovoltaic Solar Module Integrated with a Passive Cooling System

Saeed Rubaiee and M. A. Fazal *

Department of Mechanical and Materials Engineering, University of Jeddah, P.O. Box 80327, Jeddah 21589, Saudi Arabia

* Correspondence: fazal@uj.edu.sa

Abstract: The thermal regulation of a silicon photovoltaic (PV) solar system is essential as the module surface temperature beyond 25 °C deteriorates its Power Conversion Efficiency (PCE). The intensity of solar radiation seems to have a crucial impact on the PCE of a PV solar system. The present study aims to assess the effect of solar radiation variations on the PCEs of PV modules integrated with and without passive cooling systems. The used passive cooling systems are (a) multi-pipe copper frame filled with Phase Change Material (PCM) and (b) multi-pipe copper frame filled with ZnO-doped PCM. The tests were conducted at the University of Jeddah in the month of March at various local times. The results show that the ambient and module surface temperatures are directly dominated by solar radiations. The conventional PV solar system presents a higher module surface temperature as compared to that of a PV system integrated with ZnO/PCM. The enhanced module surface temperature decreases the open circuit voltage (V_{oc}) and slightly increases the short circuit current (I_{sc}) indicating its reduced electric efficiency.

Keywords: photovoltaic system; electrical efficiency; ZnO powder; PCM; solar radiation



Citation: Rubaiee, S.; Fazal, M.A. The Influence of Various Solar Radiations on the Efficiency of a Photovoltaic Solar Module Integrated with a Passive Cooling System. *Energies* **2022**, *15*, 9584. <https://doi.org/10.3390/en15249584>

Academic Editors: Carlo Renno, Philippe Leclère, Valery Meshaklin, Petros Groumpos, Chirag Bhimani and Alla Kravets

Received: 14 November 2022

Accepted: 15 December 2022

Published: 16 December 2022

Publisher's Note: MDPI stays neutral with regard to jurisdictional claims in published maps and institutional affiliations.



Copyright: © 2022 by the authors. Licensee MDPI, Basel, Switzerland. This article is an open access article distributed under the terms and conditions of the Creative Commons Attribution (CC BY) license (<https://creativecommons.org/licenses/by/4.0/>).

1. Introduction

The photovoltaic (PV) system generates electricity directly from sunlight by means of the photovoltaic effect. However, a major part of the sunlight produces heat in the PV module during this conversion process. The temperature of the module surface is enhanced due to the generated heat. The Power Conversion Efficiency (PCE) of the PV module is largely influenced by its module surface temperature [1] as well as solar radiation [2]. In recent years, several studies have been conducted to improve the Power Output (PO) through mitigation of the PV module's overheating problem by using various cooling methods. The cooling methods used so far include natural and forced air cooling [3,4], water cooling [5,6], hydraulic or refrigerant cooling [7,8], thermoelectric cooling [9,10], integration of PCM [11,12], nano-fluids [13,14], etc. The efforts paid by different researchers in increasing the PV efficiency through stabilizing the module surface temperature vary not only within any specific window, such as active or passive cooling systems, but also over a wide range of parameters. However, the sustainable achievement in stabilizing the PV module surface temperature with different approaches seems far from being complete.

The active cooling systems require extra or parasitic energy to drive the heat transfer fluids such as air, water, nano-fluids, etc., at the back or front of the PV module. It needs proper design and temperature monitoring techniques. On the other hand, the passive cooling system is driven by the nature, which is mostly based on air, liquid, and PCM [15]. In this case, heat is transferred by natural conduction, convection, and radiation mechanisms. Among others, the PCM-based passive cooling system shows some positive features including PV temperature regulation, high heat absorption, high heat absorption rate with small quantities of materials, no electricity consumption, no moving parts, and

no maintenance cost. Hachem et al. [16] reported that the use of white petroleum jelly with a PV solar system under the climate of Al-Khyara, West Bekaa of Lebanon, increased electricity yield by around 3%. According to Hasan et al. [17], the use of paraffin wax with a PV solar system under the climate of UAE improved 5.9% electric efficiency. Park et al. [18] investigated the effect of the PCM on the vertical PV solar system under the climatic condition of South Korea. They observed a 3–4 °C drop in PV surface temperature, which ultimately results in 3% improvement in energy efficiency [19]. It is obvious that the effectiveness of PCM depends on its physical properties as well as the PV system's design, location, and weather conditions.

Although many researchers have turned more attention to the PV/PCM technology and published a good number of papers in this field, its practical application is far from implementation because of some limitations with PCM. As stated by Qureshi et al. [20], the low thermal conductivity of PCM may cause slow heat transfer as well as low heat storage and release rate, which appear as major drawbacks for the practical applications. With an interest to improve the thermal performance of PV/PCM, most of the studies conducted so far have added different nanoparticles, metal powders, or fins in PCM. Wang et al. [21] incorporated 1% TiO₂ nanoparticles in paraffin wax and observed the improvement of latent heat capacity. A significant improvement of the latent heat capacity of PCM has also been reported by Babapoor and Karimi [22] upon the addition of different metal oxides nanoparticles such as SiO₂, ZnO, Al₂O₃, Fe₂O₃. However, the technical difficulties, along with encapsulation, materials selection, and design, have appeared as major challenges in this regard. In the present study, two passive cooling systems have been developed by using copper multi-pipe cooling frames, PCM, and ZnO powder. The aims of this study are to determine and compare the PCEs of different PV modules integrated with and without passive cooling systems at different times of the day under various solar radiations.

2. Materials and Methods

The tests were conducted at the University of Jeddah in the month of March by using PV modules integrated with and without passive cooling systems for various times over the test day starting from 9:00 a.m. to 4:00 p.m. Two passive cooling systems were developed by using two similar multi-pipe copper frames. One frame was filled with PCM, and the other one was filled with ZnO (1 wt%) and PCM. The used copper pipe with a diameter of 1.9 cm and wall thickness of 0.09 cm was cut to fit at the back of the PV module. Each pipe was pressed diametrically around 2 mm along with its full length, and then one end of each pipe was sealed by using silicone sealant. The multi-pipe copper frame shown in Figure 1a was made by attaching the copper pipes in parallel with two similar low carbon steel supports. High temperature adhesive was used to attach 12 pipes to the support by keeping all the sealed ends at the bottom side. The PCM (paraffin wax) was melted and poured into the pipes of the frame and then sealed at the pouring side too. The frame is then attached at the back of the PV as shown in Figure 1b to make it a PV system integrated with PCM. Similarly, another frame was filled with ZnO-doped PCM and then attached at the back of the PV solar module to make it a PV system integrated with ZnO and PCM. The specification of the used PV module (50 W each) is presented in Table 1. The other required materials including paraffin wax, ZnO powder, copper pipe, high temperature adhesive (glue), silicone sealant, glass beaker (6 mL each), etc., are purchased from a local market in the Jeddah city, Saudi Arabia.

The PV system with single PV module is placed by facing south direction with a tilt angle of about 25 °C. It is worth mentioning that the optimum tilt angle for the month of March in Jeddah is approximately 25 °C [2]. The experimental parameters to be examined include solar irradiation, air temperature, module surface temperature, wind speed, open circuit voltage, short circuit current, output power, and electrical efficiency of each PV setup. The accuracy level of used equipment is illustrated in Table 2.

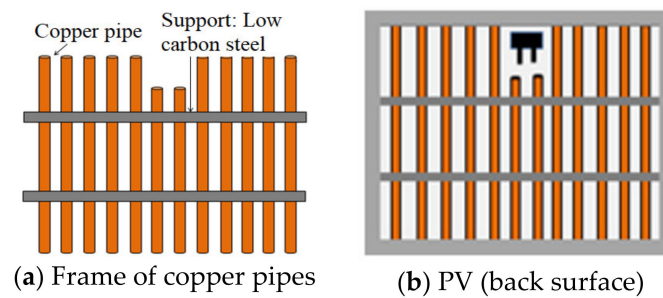


Figure 1. (a) Copper multi-pipe cooling frame, (b) PV integrated with passive cooling system.

Table 1. Specification of the PV modules supplied by the manufacturer.

Parameters	Symbol	Value
PV Dimension (mm)	$L \times W \times t$	$670 \times 550 \times 30$
Maximum power	P_{max}	50 W
Rated voltage	V_{mp}	17.8 V
Rated current	I_{mp}	2.78 A
Open circuit voltage	V_{oc}	21.8 V
Short circuit current	I_{sc}	3.11 A
Test condition (Irradiance and Cell Temperature)		$1000 \text{ W/m}^2, 25 \text{ }^\circ\text{C}$

Table 2. List of the used equipment and their accuracy levels.

Equipment	Measurement	Accuracy
Solar meter	Sun radiation	$\pm 0.38 \text{ W/m}^2/^\circ\text{C}$
Voltmeter	Open circuit voltage	$\pm 0.05\% \text{ V}$
Ammeter	Short circuit current	$\pm 0.05\% \text{ V}$
Temperature sensor	Panel surface temperature	$\pm 0.14 \text{ }^\circ\text{C}$
Digital Anemometer	Wind velocity	$\pm 0.1 \text{ m/s}$
Digital Anemometer	Atmospheric temperature	$\pm 0.2 \text{ }^\circ\text{C}$

Each PV setup is operated over a wide range of voltage and current for finding the maximum power output (P_m) and then PCE for a particular level of irradiation. The resistive load at that particular irradiation is increased from zero (short circuit) to a significantly high value (Open circuit) to determine the maximum power point by plotting I-V curve as shown in Figure 2. The maximum power output (P_m) is obtained from the maximum power point of the I-V curve. The value of PCE is determined by using Equation (1). The incident power (P_i) is determined by the product of the PV module surface area A_m in m^2 and the incident solar radiation energy (E) in W/m^2 . The value of solar radiation (E) is obtained from solar meter. The short circuit current and open circuit voltage as shown in I-V curve are denoted by I_{sc} and V_{oc} , respectively. The voltage and current at maximum power point (P_m) are presented by I_{MPP} and V_{MPP} , respectively. The maximum power out (P_m) is the area of the product of maximum current (I_{MPP}) and maximum voltage (V_{MPP}) obtained at P_m . These values are used to calculate the fill factor (FF) by using Equation (2). The final form of PCE is presented by Equation (3).

$$\text{Power conversion efficiency } (\eta) = \frac{P_m}{P_i} = \frac{P_m}{E \times A_m} \quad (1)$$

$$\text{Fill factor } (FF) = \frac{P_m}{I_{sc} \times V_{oc}} = \frac{V_{MPP} \times I_{MPP}}{I_{sc} \times V_{oc}} \quad (2)$$

$$\begin{aligned}
 \text{Power conversion efficiency } (\eta) &= \frac{P_m}{P_i \times A_m} \\
 &= \frac{V_{MPP} \times I_{MPP}}{E \times A_m} \\
 &= \frac{FF \times I_{sc} \times V_{oc}}{E \times A_m}
 \end{aligned}
 \tag{3}$$

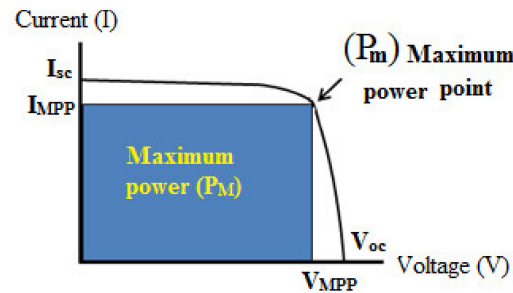


Figure 2. The I-V curve for PV solar system.

3. Results

Figure 3 presents the variation of solar radiation, ambient temperature, and wind speed with respect to time over the test day, from 9:00 a.m. to 4:00 p.m. The trend of the ambient temperature change follows the change in solar radiation indicating direct dominance of the ambient temperature by the solar radiation. However, the wind speed shown in Figure 3b varies randomly over time and does not follow the pattern of solar radiation. With the increase of solar radiation, the ambient temperature is found to increase until 12:00 p.m., and then the temperature and the solar radiation decrease with similar trends. The ambient temperature (33.3 °C) and the radiation (955 W/m²) are found to be maximized at 12:00 p.m. The variation in ambient temperature is directly caused by solar radiation, whereas the wind speed, location, and season have indirect influence on it.

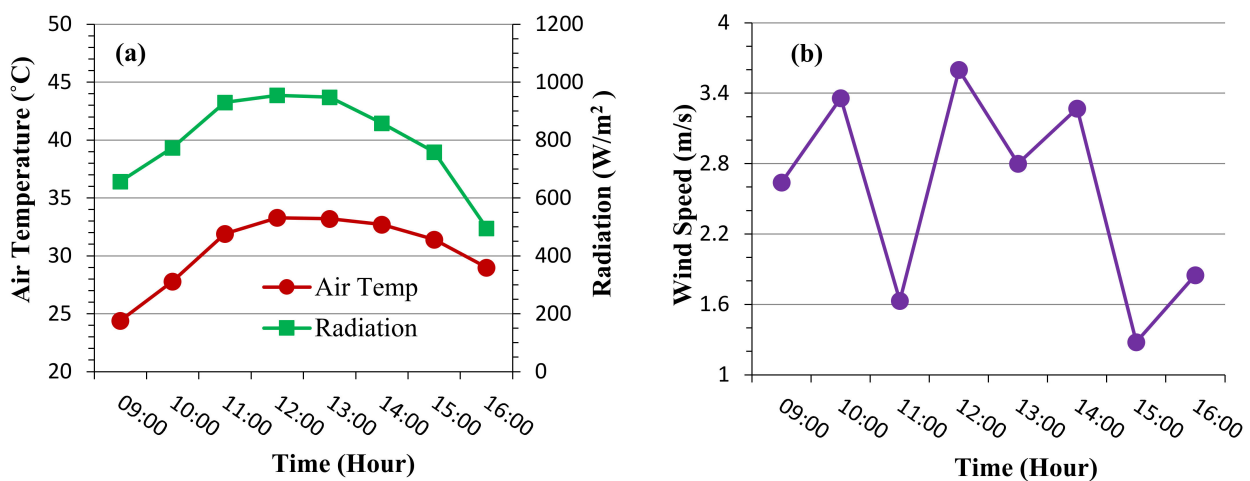


Figure 3. Variations of (a) solar radiation, ambient temperature, and (b) wind speed in the month of March in Jeddah.

Figure 4 illustrates the impacts of PCM and ZnO-doped PCM on I-V curves (a,c,e) and power outputs (b,d,f). The presented data are obtained at (a,b) 10:00 a.m. under 27.8 °C ambient temperature and 773.4 W/m² solar radiation, (c,d) 12:00 p.m. under 33.3 °C ambient temperature and 955 W/m² solar radiation, (e,f) 3:00 p.m. under 31.4 °C ambient temperature and 759 W/m² solar radiation. The maximum output power (43.04 W) of the PV system integrated with ZnO-doped PCM at 12:00 p.m. is found to be higher than those

of the conventional PV system (40.47 W) and the PV system integrated with PCM (41.68 W). This indicates that the presence of ZnO in PCM has enhanced its cooling capability. Similar effects are also observed at 10:00 a.m. and 3:00 p.m.

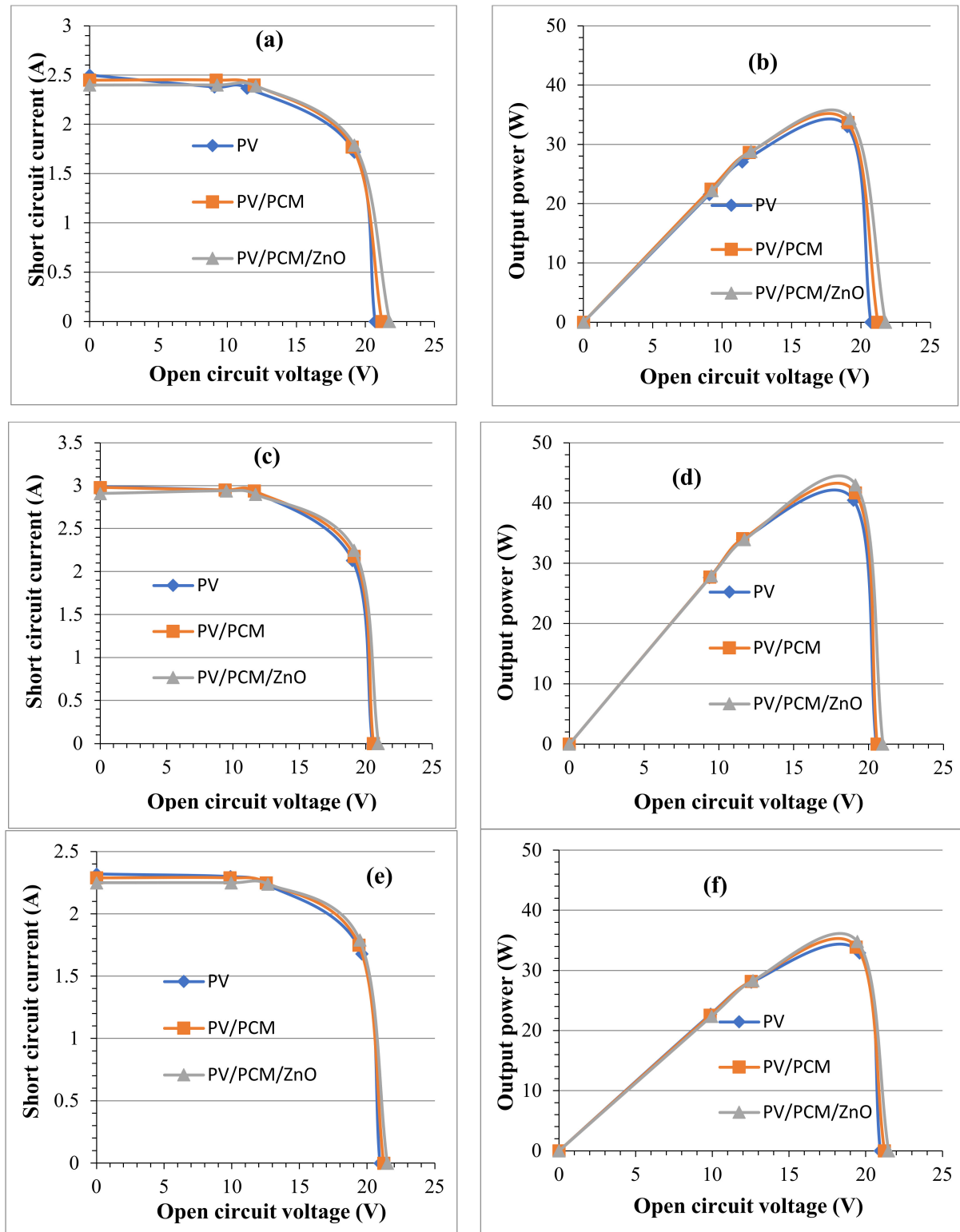


Figure 4. Plots of I-V curves (a,c,e) and variation of power outputs (b,d,f) for the PV systems in the presence and absence of PCM and ZnO-doped PCM at 10:00 a.m. (a,b), 12:00 p.m. (c,d), and 3:00 p.m. (e,f).

Figure 5 illustrates the variation of the module surface temperature with respect to the test time for different PV systems. It is seen that the surface temperature is gradually increased from 9:00 a.m. to 12:00 p.m. and then reduced until 16:00 p.m. The maximum surface temperatures of the PV system and the ZnO-doped PCM integrated PV system are found to be 53.6 °C and 50.8 °C, respectively, at 12:00 p.m. This demonstrates that the attachment of a copper multi-pipe system with ZnO-doped PCM decreases the temperature by around 2.8 °C, which is an approximately 5.22% reduction from the PV module surface temperature.

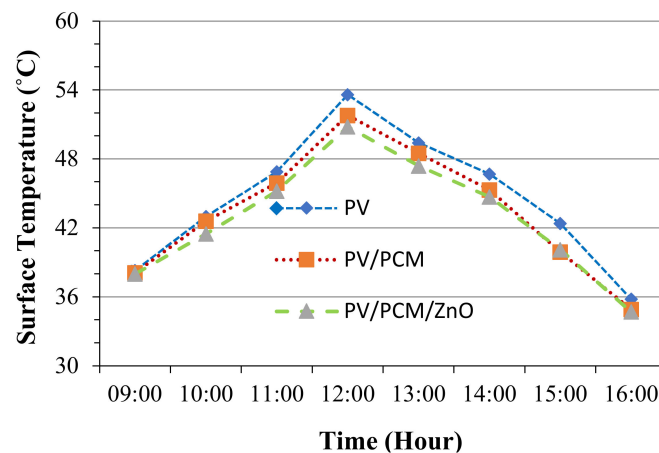


Figure 5. Variation of module surface temperature of the PV, PV with PCM, and PV with ZnO-doped PCM.

Figure 6 reveals that the efficiency of the conventional PV module is 12.69% under the radiation of 773.4 W/m^2 at 12:00 p.m. Under similar conditions, the PV system integrated with ZnO/PCM shows an electric efficiency of 12.94% with a filling factor, $FF = 73.33\%$, an open circuit voltage, $V_{oc} = 20.95 \text{ V}$, a short circuit current, $I_{sc} = 2.91 \text{ A}$. The high value of the electrical efficiency observed for the PV system integrated with ZnO-doped PCM demonstrates that the ZnO/PCM-integrated PV system can effectively reduce the adverse effect of module surface temperature. Although the ambient temperature and module surface temperature were found to be high at 12:00 p.m., the efficiencies at this noon time presented in Figure 6 are found to be higher than those at 10:00 a.m. and 3:00 p.m. In fact, this feature leads to a better and controlled thermal output during the application period of the PV solar system.

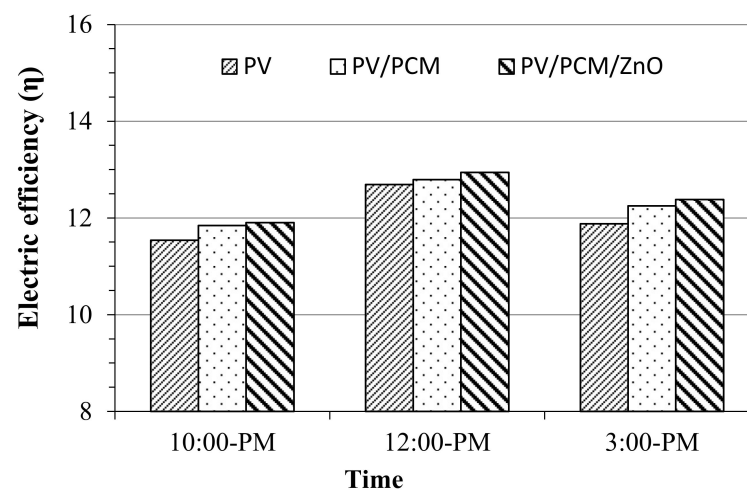


Figure 6. Conversion efficiency of different PV systems obtained at 10:00 a.m., 12:00 p.m., and 3:00 p.m.

Table 3 presents the values of module surface temperature (T_s), open circuit voltage (V_{oc}), short circuit current (I_{sc}), and efficiency (η) determined for a photovoltaic (PV) system and a PV system integrated with ZnO-doped PCM under various solar radiations at three different times, viz., 10:00 a.m., 12:00 p.m., and 3:00 p.m. At 10:00 a.m., 12:00 p.m., and 3:00 p.m., the solar radiations are found to be 773.4, 955, 759 W/m², and the module surface temperatures of PV system are identified as 43 °C, 53.6 °C, and 42.4 °C, respectively. Under these conditions, the electric efficiencies of PV systems are observed to be 11.48%, 12.69%, and 11.88%, and the power outputs (PO) are found to be 33.02 W, 40.47 W, and 32.93 W, respectively. This clearly demonstrates that the conversion efficiencies, module surface temperatures, and power outputs are directly controlled by the solar radiations. Similar trends are also found for the PV system integrated with ZnO-doped PCM. As the temperature of the PV module increases under a particular solar radiation, its power generation and efficiencies are dropped significantly.

Table 3. Ambient temperature (T_a), module surface temperature (T_s), open circuit voltage (V_{oc}), short circuit current (I_{sc}), and efficiency (η) of photovoltaic (PV) and PV integrated with ZnO-doped PCM at 10:00 a.m., 12:00 p.m., and 3:00 p.m. under different solar radiations (R).

	10:00 a.m. ($T_a = 27.8$ °C)		12:00 p.m. ($T_a = 33.3$ °C)		3:00 p.m. ($T_a = 31.4$ °C)	
	PV	PV/PCM/ZnO	PV	PV/PCM/ZnO	PV	PV/PCM/ZnO
T_s	38.3 °C	38 °C	53.6 °C	50.8 °C	42.4 °C	40.1 °C
V_{oc}	20.7 V	21.75 V	20.5 V	20.95 V	20.94 V	21.48 V
I_{sc}	2.5 A	2.4 A	2.99 A	2.91 A	2.32 A	2.25 A
η	11.48 %	11.9 %	12.69 %	12.94 %	11.88 %	12.38 %
PO	33.02 W	33.72 W	40.47 W	43.04 W	32.93	34.82
R	773.4 W/m ²		955 W/m ²		759 W/m ²	

4. Discussions

As per Figure 6, the PV module surface temperature is enhanced from 38.3 °C to 53.6 °C when the time is increased from 10:00 a.m. to 12:00 p.m. The surface temperature of the PV system is then reduced to 42.4 °C at 3:00 p.m. The observed V_{oc} , I_{sc} , and η for the PV system are found to be 20.7 V, 2.5 A, and 11.48% at 10:00 a.m.; 20.5 V, 2.99 A, and 12.69% at 12:00 p.m.; and 20.94 V, 2.32 A, and 11.88% at 3:00 p.m., respectively. It is clearly noticed that the enhancement of the module surface temperature decreases the V_{oc} and slightly increases the I_{sc} . These changes consequently reduce electrical efficiency as a result of increasing the module surface temperature. However, the module surface temperature is found to be directly dominated by the solar radiation. Similar phenomena are also observed for the PV systems integrated with ZnO-doped PCM.

It is also noted from Figure 5 that the PV system's surface temperature at 12:00 p.m. is reduced from 53.6 °C to 50.8 °C due to the integration of 1% ZnO-doped PCM at the back of the PV module. As a result, the electrical efficiency of the PV system is improved from 12.69% to 12.94% when the PV system is integrated with ZnO-doped PCM. Senthilraja et al. [23] observed an increment of electrical efficiency for a PV system from 7.5% to 8% at 12:00 p.m. due to the integration of the air-cooling system with a 0.011 kg/s mass flow rate. Similar trends are also reported by Liang et al. [24] and Sardarabadi et al. [13]. In such cases, the reduction of the cell temperature is one of the important contributing factors for enhancing electrical efficiency. An increment of the module surface temperature after passing a certain value leads to a reduction in the open circuit voltage and a slight increase in the short circuit current. The reason for this slight increment of the short circuit current with the temperature could be due to the reduced band gap energy and an increased number of photons with the required energy which create electron–hole pairs. However, the open circuit voltage decreases with the increase of temperature. According to Senthilraja et al. [23], the diffusion length of the semiconductor at higher temperatures is increased due to more output current and less output voltage, and ultimately, electrical

efficiency is reduced. Solar radiation is a major influencing factor in changing the ambient temperature and the module surface temperature. It is important to understand the mechanism in decreasing the voltage and increasing the current with the increase of the module surface temperature. Further studies should be conducted to investigate the effect of the temperature and the diffusion length of the PV materials on the voltage and current variations. Among others, the important factors that may influence the PV efficiency are wind speed, air temperature, solar peak time, air-mass, zenith angle, slope angle, dust level, and the materials of the solar module. It is worth mentioning that wind speed has a positive impact on the electrical efficiency of the PV system as it helps reduce surface temperature.

5. Conclusions

The following conclusions are drawn from the present study:

- (i) The module surface temperature is significantly dominated by solar radiation. Under any specific solar radiation, the PV efficiency and power output are improved when the module surface temperature is reduced by integrating the cooling system.
- (ii) The reduction in module surface temperature due to the addition of PCM is found to be low. This could be attributed to its low heat conductivity. However, reduction of module surface temperature is found to be high when PCM is doped with ZnO.
- (iii) At noon, the PV system integrated with ZnO/PCM drops the module surface temperature approximately 2.08 °C, indicating a 5.22% temperature reduction. It enhances electrical efficiency from 12.69% to 12.94%.
- (iv) The enhancement of the module surface temperature decreases the V_{oc} and slightly increases the I_{sc} current. The absolute value of the voltage change is more than that of the current, and, thus, it reduces the electrical efficiency of the PV system.
- (v) The mechanism of voltage reduction and current increment with the enhancement of the module surface temperature is not clearly understood. Further studies should be conducted to understand the effect of temperature and diffusion length of the PV materials in changing voltage and current.

Author Contributions: S.R.: Project administration, Writing—Reviewing and Editing, Validation; M.A.F.: Conceptualization, Project administration, Methodology, Writing—Original draft preparation. All authors have read and agreed to the published version of the manuscript.

Funding: This research was funded by Deanship of Scientific Research (DSR), University of Jeddah, Jeddah. Grant No. UJ-02-004-ICGR.

Conflicts of Interest: The authors declare no conflict of interest.

Abbreviations

c-Si	Crystalline silicon
FF	Fill factor
I_{sc}	Short circuit current
MPP	Maximum power point
PCE	Power conversion efficiency
PCM	Phase change material
PV	Photovoltaic
PV/PCM	PV integrated with PCM
PO	Power output
V_{oc}	Open circuit voltage

References

1. Sultan, S.M.; Tso, C.P.; Ervina Efzan, M.N. A new approach for photovoltaic module cooling technique evaluation and comparison using the temperature dependent photovoltaic power ratio. *Sustain. Energy Technol. Assess.* **2020**, *39*, 100705. [[CrossRef](#)]
2. Kaddoura, T.O.; Ramli, M.A.M.; Al-Turki, Y.A. On the estimation of the optimum tilt angle of PV panel in Saudi Arabia. *Renew. Sustain. Energy Rev.* **2016**, *65*, 626–634. [[CrossRef](#)]
3. Al-Waeli, A.H.A.; Sopian, K.; Kazem, H.A.; Chaichan, M.T. Photovoltaic/Thermal (PV/T) systems: Status and future prospects. *Renew. Sustain. Energy Rev.* **2017**, *77*, 109–130. [[CrossRef](#)]
4. Elminshawy, N.A.S.; Mohamed, A.M.I.; Morad, K.; Elhenawy, Y.; Alrobaian, A.A. Performance of PV panel coupled with geothermal air cooling system subjected to hot climatic. *Appl. Therm. Eng.* **2019**, *148*, 1–9. [[CrossRef](#)]
5. Moharram, K.A.; Abd-Elhady, M.S.; Kandil, H.A.; El-Sherif, H. Enhancing the performance of photovoltaic panels by water cooling. *Ain. Shams Eng. J.* **2013**, *4*, 869–877. [[CrossRef](#)]
6. Sathe, T.M.; Dhoble, A.S. A review on recent advancements in photovoltaic thermal techniques. *Renew. Sustain. Energy Rev.* **2017**, *76*, 645–672. [[CrossRef](#)]
7. Sargunanathan, S.; Elango, A.; Mohideen, S.T. Performance enhancement of solar photovoltaic cells using effective cooling methods: A review. *Renew. Sustain. Energy Rev.* **2016**, *64*, 382–393. [[CrossRef](#)]
8. Bahaidarah, H.M.S.; Baloch, A.A.B.; Gandhidasan, P. Uniform cooling of photo-voltaic panels: A review. *Renew. Sustain. Energy Rev.* **2016**, *57*, 1520–1544. [[CrossRef](#)]
9. Makki, A.; Omer, S.; Sabir, H. Advancements in hybrid photovoltaic systems for enhanced solar cells performance. *Renew. Sustain. Energy Rev.* **2015**, *41*, 658–684. [[CrossRef](#)]
10. Shukla, A.; Kant, K.; Sharma, A.; Biwole, P.H. Cooling methodologies of photovoltaic module for enhancing electrical efficiency: A review. *Sol. Energy Mater. Sol. Cells* **2017**, *160*, 275–286. [[CrossRef](#)]
11. Yao, J.; Xua, H.; Daia, Y.; Huang, M. Performance analysis of solar assisted heat pump coupled with build-in PCM heat storage based on PV/T. panel. *Sol. Energy* **2020**, *197*, 279–291. [[CrossRef](#)]
12. Stropnik, R.; Stritih, U. Increasing the efficiency of PV panel with the use of PCM. *Renew. Energy* **2016**, *97*, 671–679. [[CrossRef](#)]
13. Sardarabadi, M.; Passandideh-Fard, M.; Maghrebi, M.; Ghazikhani, M. Experimental study of using both ZnO/water nanofluid and phase change material (PCM) in photovoltaic thermal systems. *Sol. Energy Mater. Sol. Cells* **2017**, *161*, 62–69. [[CrossRef](#)]
14. Shah, T.R.; Ali, H.M. Applications of hybrid nanofluids in solar energy, practical limitations and challenges: A critical review. *Sol. Energy* **2019**, *183*, 173–203. [[CrossRef](#)]
15. Nizetic, S.; Papadopoulos, A.M.; Giama, E. Comprehensive analysis and general economic-environmental evaluation of cooling techniques for photovoltaic panels, Part 1: Passive cooling techniques. *Energy Convers. Manag.* **2017**, *149*, 334–354. [[CrossRef](#)]
16. Hachem, A.; Abdulhay, B.; Ramadan, M.; Hage, H.E.I.; Rab, M.G.E.I.; Khaled, M. Improving the performance of photovoltaic cells using pure and combined phase change materials—Experiments and transient energy balance. *Renew. Energy* **2017**, *107*, 567–575. [[CrossRef](#)]
17. Hasan, A.; Sarwar, J.; Alnoman, H.; Abdelbaqi, S. Yearly energy performance of a photovoltaic-phase change material (PV-PCM) system in hot climate. *Sol. Energy* **2017**, *146*, 417–429. [[CrossRef](#)]
18. Park, J.; Kim, T.; Leigh, S.B. Application of a phase-change material to improve the electrical performance of vertical-building-added photovoltaics considering the annual weather conditions. *Sol. Energy* **2014**, *105*, 561–574. [[CrossRef](#)]
19. Japs, E.; Sonnenrein, G.; Krauter, S.; Vrabec, J. Experimental study of phase change materials for photovoltaic modules: Energy performance and economic yield for the EPEX spot market. *Sol. Energy* **2016**, *140*, 51–59. [[CrossRef](#)]
20. Qureshi, Z.A.; Ali, H.M.; Khushnood, S. Recent advances on thermal conductivity enhancement of phase change materials for energy storage system: A review. *Int. J. Heat Mass Transf.* **2018**, *127*, 838–856. [[CrossRef](#)]
21. Wang, J.; Xie, H.; Guo, Z.; Guan, L.; Li, Y. Improved thermal properties of paraffin wax by the addition of TiO₂ nanoparticles. *Appl. Therm. Eng.* **2014**, *73*, 1541–1547. [[CrossRef](#)]
22. Babapoor, A.; Karimi, G. Thermal properties measurement and heat storage analysis of paraffin nanoparticles composites phase change material: Comparison and optimization. *Appl. Therm. Eng.* **2015**, *90*, 945–951. [[CrossRef](#)]
23. Senthilraja, S.; Gangadevi, R.; Marimuthu, R.; Baskaran, M. Performance evaluation of water and air based PVT solar collector for hydrogen production application. *Int. J. Hydrog. Energy* **2020**, *45*, 7498–7507. [[CrossRef](#)]
24. Liang, R.; Zhang, J.; Ma, L.; Li, Y. Performance evaluation of new type hybrid photovoltaic/thermal solar collector by experimental study. *Appl. Therm. Eng.* **2015**, *75*, 487–492. [[CrossRef](#)]